2014 IEEE 28th International Conference on Advanced Information Networking and Applications

End-to-end measurement of hop-by-hop available bandwidth

Kazumasa Koitani, Go Hasegawa and Masayuki Murata
Graduate School of Information Science and Technology, Osaka University, Japan
{*k-koitani, hasegawa, murata*}*@ist.osaka-u.ac.jp*

***Abstract*—Existing techniques for measuring available bandwidth measure the available bandwidth at bottlenecks along the path, and most of them do not specify the bottleneck location. In this paper, we propose an end-to-end measurement method for the hop-by-hop available bandwidth along a network path. Such a technique can facilitate advanced traffic control, especially in heterogeneous network environments. The proposed method assumes a situation where intermediate routers can record the arrival and departure times of incoming packets as timestamps in the packets themselves. The endhost sends probe packets at various rates and estimates the available bandwidth at each network section using the incoming and outgoing rates of packets calculated from intermediate timestamps, based on statistical processing under a fluid traffic model.**

We present extensive simulation results for the proposed method and confirm that it can accurately measure the available bandwidth of each section along the network path even when the available bandwidth of the sender-side network is smaller than that of the receiver-side network.

***Keywords*-Available bandwidth, active probing, end-to-end measurement, traffic control**

I. Introduction

The available bandwidth of an end-to-end network path is determined by bottlenecks, which are the section with the smallest available bandwidth along the path. Many tools for measuring the available bandwidth of an end-to-end network path are proposed [1]–[8] and evaluated [9]–[11]. These bandwidth measurement tools can determine the available bandwidth at bottlenecks, but with the exception of*pathneck* [12], none of them can determine the location of the bottlenecks along the path. However, knowing the locations of bottlenecks may enhance the quality of network applications. For example, in overlay networks for video and voice conferencing, when an endhost determines the location of a bottleneck link, the endhost can enhance the application quality by adding or deleting overlay nodes to the overlay network to change the route between endhosts. Another example is network control in wired-cum-wireless network environments, where a wireless client terminal can control the data transmission rate of the wireless network according to the measured bandwidth of the wired part. However, to our knowledge, there has been no previous research on such end-to-end measurement of the available bandwidth of multiple sections of the network path.

In this paper, we propose an end-to-end measurement method for the hop-by-hop available bandwidth of a network path. The proposed method estimates the available bandwidth based on the assumption that some intermediate routers along the path can record the arrival and departure times of traversing packets as timestamps in the packets themselves. We divide the end-to-end path into multiple sections at such intermediate routers and estimate the available bandwidth of each section simultaneously by observing the intervals of incoming and outgoing packets in each section. Considering the effect of cross traffic, the endhost sends probe packets at various rates and estimates the available bandwidth based on their incoming and outgoing packet rates at each section. To estimate the available bandwidth, we construct a simple mathematical model of the relationships between incoming and outgoing packet rates.

To evaluate the performance of the proposed method, we conduct simulation experiments using ns-2 [13]. We evaluate the measurement accuracy of the proposed method under various bandwidth settings including situations where the available bandwidth of the sender-side network is smaller than that of the receiver-side network. We also evaluate the performance of the proposed method in several scenarios constructed by varying the settings of physical and available bandwidth and the hop count of the path, and verify the robustness of the proposed method.

The rest of this paper is organized as follows. Section II describes the principle of end-to-end available bandwidth measurement based on existing methods. Section III explains the principle of hop-by-hop bandwidth measurement and verifies its feasibility. Subsequently, we propose a multi-section measurement of the available bandwidth. Section IV evaluates the measurement accuracy of the proposed method in various situations. In Section V, we conclude this paper and outline the direction of future work.

II. End-to-end measurement of available bandwidth

In this section, we explain the fundamental principle of measuring the available bandwidth of an end-to-end network path. Many tools have been developed for end-to-end measurement of available bandwidth, such as Cprobe [1], Pathload [2], and pathChirp [3]. Such tools employ methods where a sender generates probe packets and sends them to a receiver at a certain rate. The receiver observes the arrival intervals of the probe packets, and determines whether or not the departure rate of probe packets is larger than the available bandwidth of the path between the sender and the receiver,

1550-445X/14 $31.00 © 2014 IEEE
DOI 10.1109/AINA.2014.9

by comparing the departure and arrival intervals of the probe packets. This process is repeated with various departure rates to determine the available bandwidth accurately. In this section, we briefly explain the mathematical background of the above method.

A. Definition of available bandwidth

We assume that the network model in this section is as illustrated in Figure 1, and that the path between the sender and the receiver is predetermined and fixed. Probe packets are sent from the sender to the receiver via routers along the path which hold the probe packets in a buffer and relay them to the receiver. The path consists of H links denoted as i ($1 \leq i \leq H$). The physical bandwidth at link i is denoted as C_i. Therefore, the physical bandwidth C of an end-to-end network path is equal to that of the link with the narrowest bandwidth, and is represented as follows.

$$C \equiv \min_{1 \leq i \leq H} C_i \tag{1}$$

The average bandwidth utilization of link i at time t is denoted as $u_i(t)$. The available bandwidth of link i at time t, denoted as $A_i(t)$, is represented as follows.

$$A_i(t) \equiv C_i(1 - u_i(t)) \tag{2}$$

Thus, the available bandwidth on a path at time t is represented as follows.

$$A(t) \equiv \min_{1 \leq i \leq H} C_i(1 - u_i(t)) \tag{3}$$

B. Existing methods and their limitations

Next, we explain the principle of determining the available bandwidth of an end-to-end network path. This principle explores the relation between one-way delay from the sender to the receiver and the departure and arrival intervals of probe packets.

The sender sends a sequence of K probe packets to the receiver. The departure time of the k th ($1 \leq k \leq K$) probe packet from the sender is denoted as t_k, and the arrival time of that packet at the receiver is denoted as t'_k. The one-way delay of the k th probe packet is denoted as $D_k = t'_k - t_k$. We focus on the difference between the one-way delays of the k th and $(k+1)$ th probe packets, which is calculated as follows.

$$\begin{aligned} \Delta D_k &= D_{k+1} - D_k \\ &= (t'_{k+1} - t_{k+1}) - (t'_k - t_k) \\ &= (t'_{k+1} - t'_k) - (t_{k+1} - t_k) \\ &= \Delta t'_k - \Delta t_k \end{aligned} \tag{4}$$

$\Delta t'_k$ in Equation (4) is the arrival interval of the k th and $(k+1)$ th probe packets at the receiver, and Δt_k is the departure interval of the corresponding packets. When the departure rate of probe packets is higher than the available bandwidth, the value of ΔD_k becomes positive since the arrival intervals become larger than the departure intervals. However, when the departure rate at the sender is equal to or lower than the available bandwidth, the value of ΔD_k is close to 0 since we can expect the interval between packets to remain unchanged when passing through the network. Note that we do not require the synchronization of clocks at the sender and the receiver to evaluate Equation (4), whereas the measurement of one-way delay requires such synchronization.

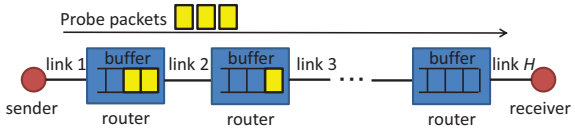

Figure 1: Network model

Therefore, by sending probe packets at a certain rate and observing their arrival times at the receiver, we can determine whether the departure rate is higher or lower than the available bandwidth. Repeating these operations allows for estimating available bandwidth of an end-to-end network path.

III. Hop-by-hop bandwidth measurement principle and proposed method

We assume that the network path between a sender and a receiver is divided into multiple sections at intermediate routers, as illustrated in Figure 2. Sections of the path from the sender are referred as the 1st, 2nd, $\cdots$, Nth network section. The physical bandwidth of the j th network section is denoted as $C(j)$, and the available bandwidth is denoted as $A(j)$, assuming that the physical and available bandwidths of each network section remain unchanged during the measurement task. We focus on measuring the available bandwidth for all network sections by using probe packets sent from the sender to the receiver.

A. Feasibility of multi-section measurement

The available bandwidth of a single network section can be measured by injecting probe packets into the network section at various rates, both higher and lower than the actual available bandwidth of that network section. When all of the injection rates of probe packets are lower than the actual available bandwidth, we cannot measure the available bandwidth accurately. Therefore, to measure the available bandwidth of all network sections along the path, we consider the following condition must be satisfied.

$$\min_{1 \leq k < j} A(k) > A(j) \ (1 \leq j \leq N) \tag{5}$$

Conversely, measuring the available bandwidth is impossible when the available bandwidth of the j th network section is smaller than that of the $(j+1)$ th network section because the rate at which probing packets leaves a certain network section is expected to be equal to or lower than

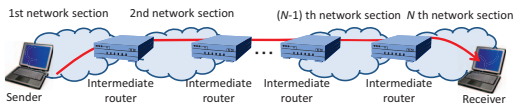

Figure 2: Network model for multi-section bandwidth measurement of the network path

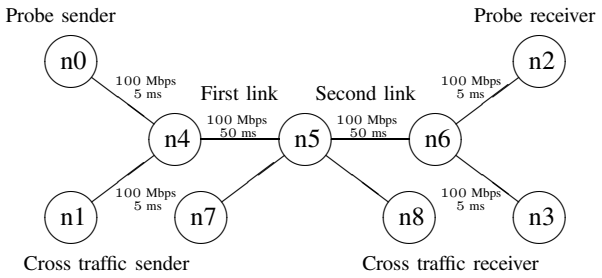

Figure 3: Network topology used in the simulation experiments in Subsection III-A

the available bandwidth of that section. However, when probing packets are injected at a sufficiently high rate, the outgoing rate would become higher than the actual available bandwidth of that network section [14]. This means that it is feasible to measure the available bandwidth of individual network sections even when Equation (5) is not satisfied. In the following subsection, we validate the feasibility of the proposed method by simulation experiments using ns-2.

Figure 3 shows the network topology used in the simulation experiments. The propagation delay of the link between n4 and n5 (First link) and that between n5 and n6 (Second link) is 50 ms, and that between all other links is 5 ms. The physical bandwidth of all links in the network is set to 100 Mbps. Cross traffic is sent from node n1 to node n8 via nodes n4 and n5 at a rate of X_1 Mbps, as well as from node n7 to node n3 via nodes n5 and n6 at a rate of X_2 Mbps. Therefore, the available bandwidth of the first link is $(100 - X_1)$ Mbps and that of the second link is $(100 - X_2)$ Mbps. The cross traffic consists of UDP packets whose departure intervals follows an exponential distribution with a given mean value. Probe packets are sent from node n0 to node n2 via nodes n4, n5, and n6, traversing the first and second links. The probe packets are sent from node n0 at intervals from 1.0×10^{-4} to 2.0×10^{-3} s in units of 1.0×10^{-5} s, which corresponds to a rate from 6 Mbps to 120 Mbps. The number of probe packets sent at a time is K. The probe packet size is set to $1,500$ Bytes and the packet size of cross traffic is set to $1,000$ Bytes. With these settings, we observe the incoming and outgoing rates of probe packets at the second link, which are taken as the averaged values over K_0 probe packets.

Figure 4 shows the simulation results for the relationship between incoming and outgoing rates of probe packets at the second link when $K_0 = 2$, 6, and 10. This graph shows the case where $X_1 = 50$ and $X_2 = 30$. Since the actual available bandwidth of the first and second links is 50 and 70 Mbps, respectively, Equation (5) is not satisfied. However, we can see from this figure that a non-negligible portion of probe packets are injected into the second link at a rate higher than 50 Mbps, regardless of the value of K_0. Also, when the incoming rate is high, the outgoing rate of probe packets tends to be lower than the incoming rate, especially if K_0 is large. This means that we can measure the available bandwidth of the second link, even though Equation (5) is not satisfied.

Next, we focus on the effect of K_0. In the case of small K_0 (Figure4(a)), there is no stable relationship between incoming and outgoing rates of probe packets. In contrast, too large a value of K_0 would result in smooth incoming and outgoing rates, which would obscure the difference between the two, as can be seen by comparing Figures 4(b) and 4(c). This may affect the measurement accuracy, which is confirmed in Section IV. Furthermore, a larger value of K_0 requires a larger number of probe packets in order to obtain a sufficient number of probing samples. Thus, when setting the value of K_0, we must consider the measurement accuracy and the number of probe samples necessary in order to obtain meaningful measurement results.

B. Proposed method

We propose a method for measuring available bandwidth of multiple sections of an end-to-end network path based on the observations in Subsection III-A. We first show the principle of the proposed method considering a difference between the measurement of the available bandwidth at the bottleneck and the multi-section measurement. Next, we describe the process of measuring the available bandwidth of arbitrary sections of a network path. Finally, we present the steps in the measurement process in detail.

1) Overview: To measure the available bandwidth of arbitrary sections of a network path, the probe packets have to arrive at each network section at a designated rate. However, this is difficult to achieve in practice for an arbitrary network section because the packet arrival intervals vary due to fluctuation in the amount of cross traffic. For this reason, the sender sends probe packets at various rates to the receiver and estimates the available bandwidth of arbitrary sections of the network path based on statistical analysis. The measurement process is as follows.

1) The sender sends probe packets to the receiver at various rates, and intermediate routers along the path record the arrival time of each probe packet as a timestamp into the packet itself.
2) When a probe packet arrives at the receiver, the receiver estimates the available bandwidth of each network

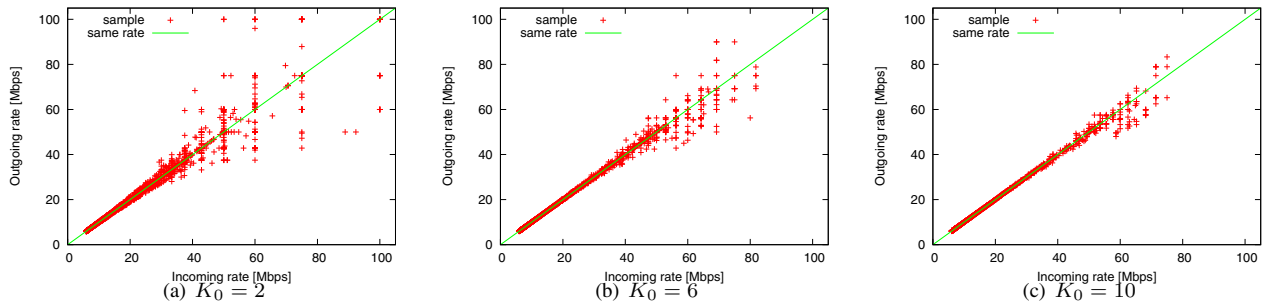

(a) $K_0 = 2$ (b) $K_0 = 6$ (c) $K_0 = 10$

Figure 4: Relationship between incoming and outgoing rates with $X_1 = 50$ and $X_2 = 30$

section based on the arrival and departure times of the probe packet for the corresponding section.

3) When the available bandwidth estimation for the entire network is complete or measurement with high accuracy seems to be impossible, the measurement procedure is terminated. Otherwise, we return to step 1.

In the following subsections, we explain steps 1 and 2 in detail.

2) Hop-by-Hop timestamps of probe packets: The bandwidth measurement method presented in this paper is based on the observation of a single pair of incoming and outgoing rates of probe packets in the network. Existing measurement methods can obtain only the available bandwidth at bottlenecks in the network. To measure the available bandwidth of multiple network sections, we assume that intermediate routers (Figure 2) can record the times at which probe packets pass through the router into the packets themselves. The proposed method utilizes those timestamps to estimate the available bandwidth of each network section. To our knowledge, routers currently deployed in real-world networks are not capable of recording timestamps into packets, but such routers are being developed [15], [16] for various end-to-end measurement purposes. Furthermore, the state-of-the-art network research trends such as Sofware Defined Network (SDN) make the availability of the timestamp capability on the network nodes becoming higher.

3) Calculation of available bandwidth based on statistical analysis: We propose a method for calculating the available bandwidth based on probing results as shown in Figure 4. The simulation results in Figure 4 can be abstracted into a simple mathematical model illustrated in Figure 5. The probing results can be divided into two regions (denoted as (i) and (ii)). In region (i), the departure rate of probe packets is lower than the actual available bandwidth. Therefore, the incoming and outgoing rates become almost equal in that region. In contrast, in region (ii), the probing packets are injected at a higher rate than the actual available bandwidth. In this case, the outgoing rate would be lower than the incoming rate. We utilize a fluid model [10] to determine the outgoing rate of probe packets from the incoming rates

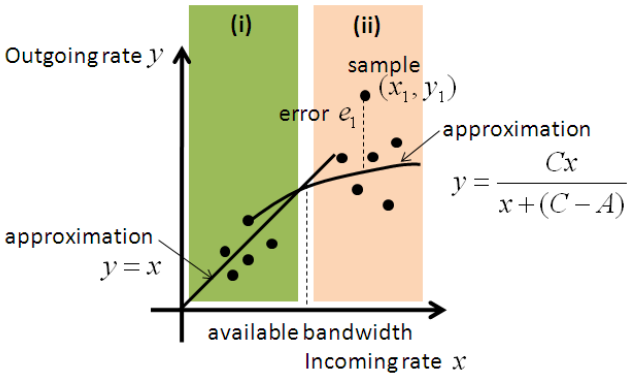

Figure 5: Computation of available bandwidth in the proposed method

and the actual available bandwidth. We denote the incoming rate of probe packets as x bps and the outgoing rate for that incoming rate as $y(x)$ bps. The physical available bandwidths are denoted as C [bps] and A [bps], respectively. Then, the model in Figure 5 can be represented as follows.

$$y(x) = \begin{cases} x & x \le A \\ \frac{Cx}{x+(C-A)} & x > A \end{cases} \tag{6}$$

The above equation is derived based on the assumption that the outgoing traffic rate at the bottleneck becomes proportional to the incoming rate.

The proposed method first gathers probing samples as shown in Figure 4 and determines the available bandwidth (which corresponds to A in Equation (6)), by simple regression of the equation to obtain a fit for all probing samples. This regression is the point where the proposed method differs from the train of packet pairs method [17]. We explain the proposed method in detail below.

The sender sends K probe packets, denoted as $P_1, P_2, \cdots, P_K$, at a certain rate. We focus on K_0 successive packets beginning with the i th packet, which corresponds to the sequence $P_i, P_{i+1}, \cdots, P_{i+K_0-1}$ $(1 \le i \le K - K_0 + 1)$. We calculate the incoming and outgoing rates from timestamps

recorded at intermediate routers, which are denoted as x_i bps and y_i bps, respectively. We define (x_i, y_i) as the i th probing sample. Note that we can obtain $(K - K_0 + 1)$ samples from K packets. We assume that the sender sends probing packets repeatedly and obtains N_{all} samples. Next, we divide these samples based on their incoming rates to obtain the average values. We set the rate resolution to R_0 bps. Then, we calculate the average incoming and outgoing rates of samples for each incoming rate. We denote the averaged samples as $(\hat{x_k}, \hat{y_k})$ $(1 \leq k \leq \lceil C(j)/R_0 \rceil)$, assuming that $C(j)$ is known in advance, and estimate the available bandwidth of the j th network section (denoted by $\bar{A}(j)$) by the equation below.

$$\bar{A}(j) = \underset{A(j)}{\operatorname{argmin}} \ e(A(j)) \tag{7}$$

where $e(A(j))$ is calculated as follows.

$$\begin{aligned} e(A(j)) \quad = \quad & \sum_{\hat{x}_i \leq A(j)} (\hat{y}_i - \hat{x}_i)^2 \\ & + \sum_{\hat{x}_i > A(j)} \left(\hat{y}_i - \frac{C(j) \cdot \hat{x}_i}{\hat{x}_i + (C(j) - A(j))} \right)^2 \end{aligned} \tag{8}$$

IV. Performance evaluation

We evaluate the performance of the proposed method by conducting simulation experiments using ns-2. First, we evaluate the fundamental performance using a 2-hop network topology considering the situation where the available bandwidth of the receiver-side network is higher than that of the sender-side network. Next, we evaluate the influence of various conditions to assess the robustness of the proposed method.

A. Fundamental evaluation of the proposed method

First, we examine the basic behavior of the proposed method with a simple network topology. The network topology (illustrated in Figure 3) is the same as in Subsection III-A. In this topology, the path between the endhosts consists of segments that are not measured (links directly connected to the endhosts) and segments that are measured (all other links). The physical bandwidth of all links is set to 100 Mbps. The available bandwidth of the first link, which is located between nodes n4 and n5, is denoted as $A(1)$, and the available bandwidth of the second link, which is located between nodes n5 and n6, is denoted as $A(2)$. We vary $A(1)$ and $A(2)$ from 10 Mbps to 90 Mbps by changing the rate of cross traffic. The timer granularity of the intermediate router is set to 1.0×10^{-6} s. In this environment, we measure the available bandwidth of the second link by the proposed method.

Figure 6 presents the simulation results for the measurement accuracy of the available bandwidth of the second link. Each graph in Figure 6 corresponds to a different value of the actual available bandwidth of the first link ($A(1)$). The graphs present the relation between actual and estimated values of the available bandwidth of the second link for $K_0 = 2$, 4, 8, 16, 32 and 47. The values of parameters K and R_0 of the proposed method are set to 50 and 1 Mbps, respectively. The center of each error bar in the graph indicates the average of the corresponding estimation result, and the width of each bar indicates 95% confidence interval.

These figures indicate that the available bandwidth of the second link is measured accurately regardless of the actual available bandwidth of the two links ($A(1)$ and $A(2)$). Especially when $A(2) < A(1)$, in which case Equation (5) is satisfied, the available bandwidth can be measured with high accuracy. When $A(2) > A(1)$, in which case Equation (5) is not satisfied, the measurement accuracy is lower but remains reasonable. However, when $A(2)$ is close to 100 Mbps, the measurement accuracy degrades, especially when $A(1)$ is small. This is due to the decrease in the number of probing samples whose incoming rate is higher than $A(2)$. Also, to obtain accurate measurement results, we should avoid setting $K_0 = 2$ since in that case the measurement results fluctuate considerably (Figure 6). This is because the relation between incoming and outgoing rates becomes unstable (Figure 4(a)).

B. Influence of physical bandwidth

We evaluate the influence of physical bandwidth on the measurement accuracy by using the same network topology as in the previous simulation experiments. The difference from the previous experimental setup is the values of the physical and available bandwidths of all links in the network. The physical bandwidth is set to 10 Mbps or 1 Gbps, and the cross traffic rates and available bandwidths are configured proportionally to the physical bandwidth.

Figures 7 and 8 present the simulation results for the available bandwidth of the second link where the physical bandwidth is set to 10 Mbps and 1 Gbps, respectively. We focus on the measurement results for the same bandwidth utilization of the first and second links in Figures 6, 7, and 8. These figures indicate that the available bandwidth can be measured accurately regardless of the physical bandwidth. In general, when the physical bandwidth is large, the measurement accuracy is low because of the timer granularity of the intermediate router. However, in the proposed method, the statistical processing can compensate for the low measurement accuracy.

C. Influence of hop count along path

Next, we evaluate the influence of the hop count along a path on the measurement accuracy. The network models are shown in Figure 9, where the number of hops between nodes connecting source and destination hosts is set to three, five, and nine. The remaining settings are the same as in the two-hop model.

The above results indicate that the measurement accuracy depends mainly on whether Equation (5) is satisfied. For this

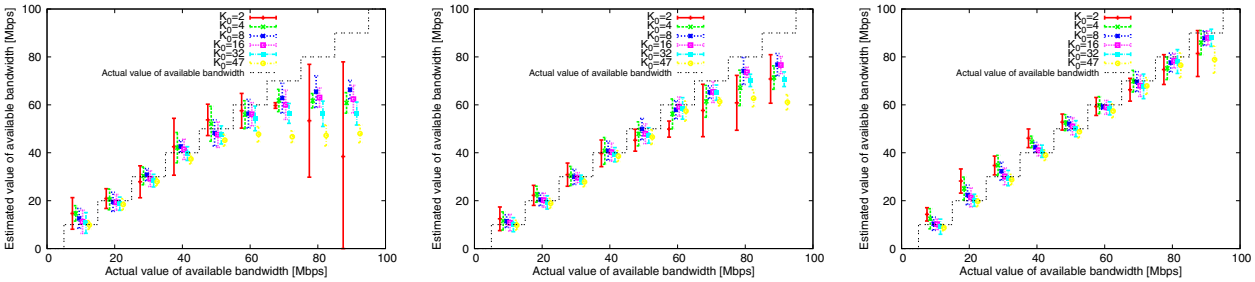

(a) $A(1) = 10$ Mbps (b) $A(1) = 50$ Mbps (c) $A(1) = 90$ Mbps

Figure 6: Estimation results with 100 Mbps of physical bandwidth

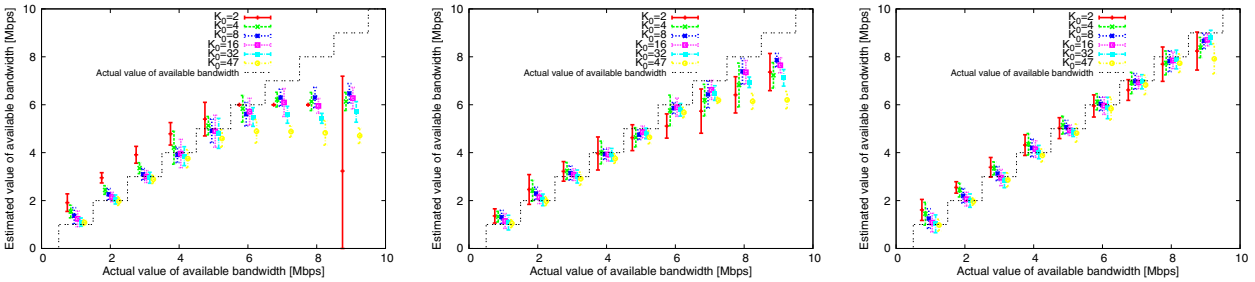

(a) $A(1) = 1$ Mbps (b) $A(1) = 5$ Mbps (c) $A(1) = 9$ Mbps

Figure 7: Estimation results with 10 Mbps of physical bandwidth

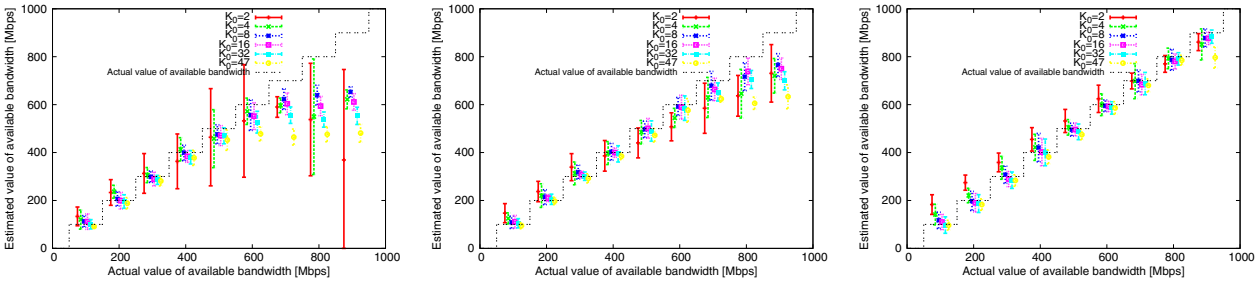

(a) $A(1) = 100$ Mbps (b) $A(1) = 500$ Mbps (c) $A(1) = 900$ Mbps

Figure 8: Estimation results with 1 Gbps of physical bandwidth

reason, we examine the following two cross traffic scenarios.

- Scenario 1: The available bandwidth decreases gradually in equal steps from the sender host to the receiver host.
- Scenario 2: The available bandwidth increases gradually in equal steps from the sender host to the receiver host.

The detailed settings for the available bandwidth are summarized in Table I. The estimation results are shown in Figures 10 and 11 for Scenarios 1 and 2, respectively. Each graph in the figures corresponds to a different hop count of the path. Figure 10 indicates that when the available bandwidth increases together with the hop count from the sender (in which case Equation (5) is satisfied), the available bandwidth can be measured accurately regardless of the total number of hop counts between the sender and the receiver. However, Figure 11 indicates that in case Equation (5) is not satisfied, the estimation accuracy degrades as the hop count from the sender increases. This occurs because when probe packets traverse multiple links with ever smaller available bandwidth, their incoming rates in the subsequent network sections decreases with higher probability.

D. Performance in case of multiple bottlenecks

Finally, we verify the performance of the proposed method in case of multiple bottleneck locations along the

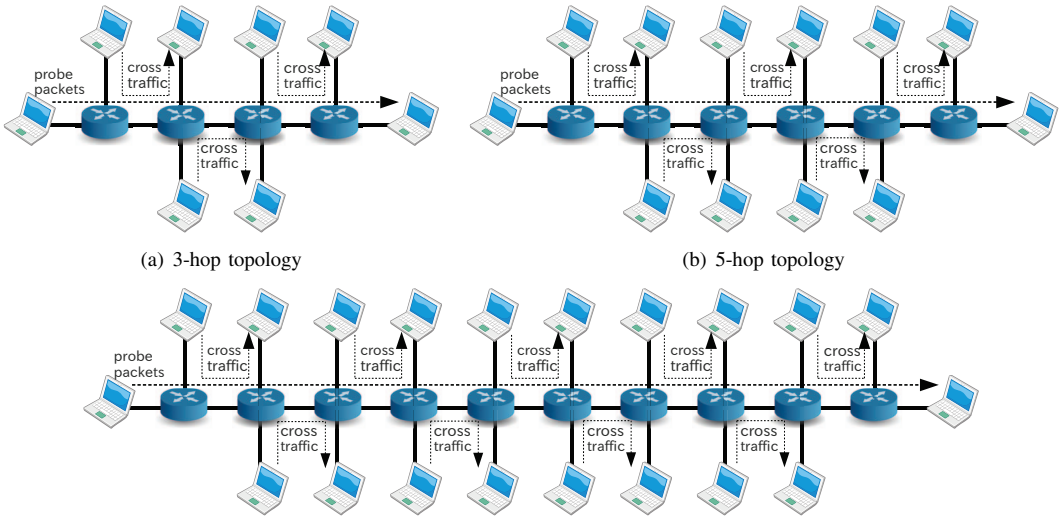

(a) 3-hop topology

(b) 5-hop topology

(c) 9-hop topology

Figure 9: Network topologies with higher hop counts

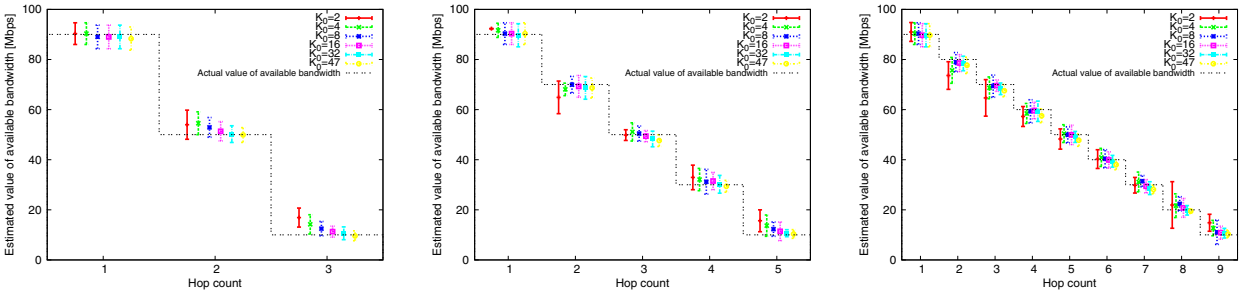

(a) 3-hop network

(b) 5-hop network

(c) 9-hop network

Figure 10: Effect of hop count in Scenario 1

Table I: Settings for the available bandwidth in 3-, 5-, and 9-hop topologies

	Scenario 1	Scenario 2
3-hop topology	(90, 50, 10) Mbps	(10, 50, 90) Mbps
5-hop topology	(90, 70, $\cdots$, 10) Mbps	(10, 30, $\cdots$, 90) Mbps
9-hop topology	(90, 80, $\cdots$, 10) Mbps	(10, 20, $\cdots$, 90) Mbps

path. We utilize the 5-hop network topology shown in Figure 9(b). The physical bandwidth of the links is set to 100 Mbps and the available bandwidth of each link from the sender is 50, 30, 50, 30, and 50 Mbps in this order. The estimation results (Figure 12) indicate that the available bandwidth of all links along the path is measured accurately and the bottleneck locations are identified correctly, suggesting that the proposed method can be applied with equal success in cases of a single or multiple bottleneck locations.

V. Conclusion and Future Work

In this paper, we proposed a method for simultaneous measurement of the available bandwidth at multiple locations along an end-to-end network path. We extended the measurement principle utilized in existing measurement tools by adding a timestamp function to intermediate routers along the path, whereby the arrival and departure times of each packet are recorded in the packet itself. We validated the performance of the proposed method by simulation experiments and found that the available bandwidth at multiple locations along the path can be measured with reasonable accuracy, even when the available bandwidth of the receiver-side network is higher than that of the sender-side network. We also validated the robustness of the proposed method for various situations.

In future work, we plan to introduce an algorithm allowing the number of probe packets to be configured in order to decrease the measurement load on the network while maintaining the measurement accuracy. Furthermore, we

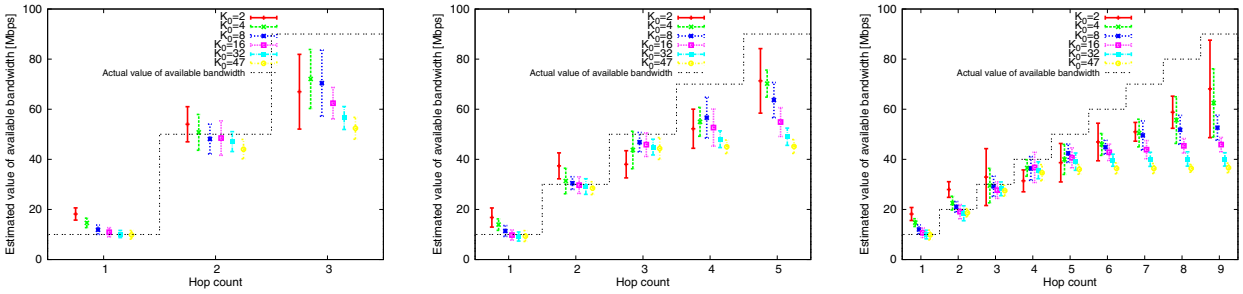

(a) 3-hop network (b) 5-hop network (c) 9-hop network

Figure 11: Effect of hop count in Scenario 2

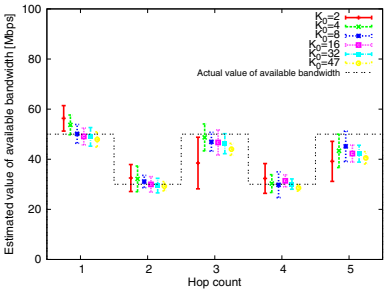

Figure 12: Estimation results in a case of multiple bottlenecks

plan to implement the proposed method and to verify its effectiveness in actual network environments.

REFERENCES

[1] C. Robert L and M. E. Crovella, "Dynamic Server Selection using Bandwidth Probing in Wide-Area Networks," tech. rep., Boston University, 1996.

[2] M. Jain and C. Dovrolis, "End-to-End Available Bandwidth: Measurement Methodology, Dynamics, and Relation with TCP Throughput," in *Proceedings of ACM SIGCOMM 2002*, pp. 295–308, August 2002.

[3] V. J. Ribeiro, R. H. Riedi, R. G. Baraniuk, J. Navratil, and L. Cottrell, "pathChirp: Efficient Available Bandwidth Estimation for Network Paths," in *Proceedings of PAM 2003*, pp. 1–11, April 2003.

[4] A. B. Downey, "Using Pathchar to Estimate Internet Link Characteristics," in *Proceedings of ACM SIGCOMM 1999*, pp. 241–250, October 1999.

[5] E. Bergfeldt, S. Ekelin, and J. M. Karlsson, "Real-time Available-Bandwidth Estimation using Filtering and Change Detection," *Computer Networks*, vol. 53, no. 15, pp. 2617–2645, October 2009.

[6] L. Lao, C. Dovrolis, and M. Y. Sanadidi, "The Probe Gap Model can Underestimate the Available Bandwidth of Multihop Paths," *ACM SIGCOMM Computer Communication Review*, vol. 36, no. 5, pp. 29–34, October 2006.

[7] X. Hei, B. Bensaou, and D. H. K. Tsang, "Model-based End-to-End Available Bandwidth Interference using Queueing Analysis," *Computer Networks*, vol. 50, no. 12, pp. 1916–1937, August 2006.

[8] T. G. Sultanov and A. M. Sukhov, "Simulation Technique for Available Bandwidth Estimation," in *Proceedings of EMS 2010*, pp. 490–495, November 2010.

[9] N. Hu and P. Steenkiste, "Evaluation and Characterization of Available Bandwidth Probing Techniques," *IEEE Journal on Selected Areas in Communications*, vol. 21, no. 6, pp. 879–894, August 2003.

[10] J. Strauss, D. Katabi, and F. Kaashoek, "A Measurement Study of Available Bandwidth Estimation Tools," in *Proceedings of IMC 2003*, pp. 39–44, October 2003.

[11] A. Shriram, M. Murray, Y. Hyun, N. Brownlee, A. Broido, M. Fomenkov, and K. Claffy, "Comparison of Public End-to-End Bandwidth Estimation Tools on High-Speed Links," in *Proceedings of PAM 2005*, pp. 306–320, March 2005.

[12] N. Hu, L. E. Li, Z. M. Mao, P. Steenkiste, and J. Wang, "Locating Internet Bottlenecks: Algorithms, Measurements, and Implications," in *Proceedings of ACM SIGCOMM 2004*, pp. 41–54, September 2004.

[13] "ns-2 web page." available at http://isi.edu/nsnam/ns/.

[14] C. Dovrolis, P. Ramanathan, and D. Moore, "What do Packet Dispersion Techniques Measure?," in *Proceedings of INFOCOM 2001*, vol. 2, pp. 905–914, April 2001.

[15] A. Machizawa, H. Toriyama, T. Iwama, and A. Kaneko, "Development of a Cascadable Passing Through Precision UDP Time-Stamping Device," *IEICE Transactions on Communications*, vol. J88-B, no. 10, pp. 2002–2011, October 2005. (in Japanese).

[16] A. Machizawa and Y. Kitaguchi, "Improvement of Software Timestamp Accuracy with Interrupt Handler and High Precision PC," *IEICE Transactions on Communications*, vol. J87-B, no. 10, pp. 1678–1685, October 2004. (in Japanese).

[17] B. Melander, M. Bjorkman, and P. Gunningberg, "A New End-to-End Probing and Analysis Method for Estimating Bandwidth Bottlenecks," in *Proceedings of GLOBECOM 2000*, vol. 1, pp. 415–421, November 2000.